

Fouling in pleated microfiltration cartridges caused by *Pseudomonas putida*

Irene Rosas, Sergio Collado, Irene Fernández, Antonio Gutierrez-Lavin, Mario Diaz

Department of Chemical Engineering and Environmental Technology, University of Oviedo, E-33071 Oviedo, Spain

Abstract

Characteristics and mechanisms of the fouling of microfiltration pleated cartridges (10-inch, PES, pore size of 0.2 μm) in biotechnical applications were analyzed, in order to obtain information about strategies that allow increasing their lifespan. Specifically, fouling experiments were carried out using the biodegradation of salicylic acid by means of *Pseudomonas putida* as model of cellular media. A complete blocking mechanism with non-uniform distribution of the fouling along the pleated structure was proposed. Main accumulation of solids was located into the space between pleats near to the external perimeter of the filter, whereas the base of the pleats remained relatively clean, only fouled by small particles that can cause a small standard blocking of the pores. Concerning fouling cures, air scouring only provoked moderate recoveries of permeability after relaxation periods of days when spaces between pleats are completely filled and the biomass began to accumulate over the pleated structure. Backflushing (30 s) effectiveness tended to decrease with operation time and consecutive applications, but improved the effect of a subsequent relaxation on the permeability recovery. After chemical cleaning, permeability recovery (R) of 87.8% was observed, which implies a considerable increase of the lifespan of the cartridge.

Keywords

Cleaning, Fouling, Microfiltration pleated cartridge, PES membrane, *P. putida*

1. Introduction

Microfiltration is a process for separating particles with diameters between 0.1 and 10 μm from suspensions by moving the liquid through a porous membrane. Microfiltration processes have found widespread use in the food and dairy industry, biotechnology (e.g. cell separation from fermentation broth) and the treatment of wastewaters [1].

Pleating of microfiltration membranes allows a larger surface area to be packed into small volume modules and is an integral feature of cartridges used in a range of biotechnology applications [2]. In a pleated cartridge, which consist of a microfiltration membrane surrounding a central perforated core (or a fabricated structure, still basically cylindrical), the flow of liquid is from the outside, through the medium and out from the axis. Suspended solids are thus removed from suspension to be deposited on the outside of the element, or in the interstices of the filter medium [3] (Fig. 1b).

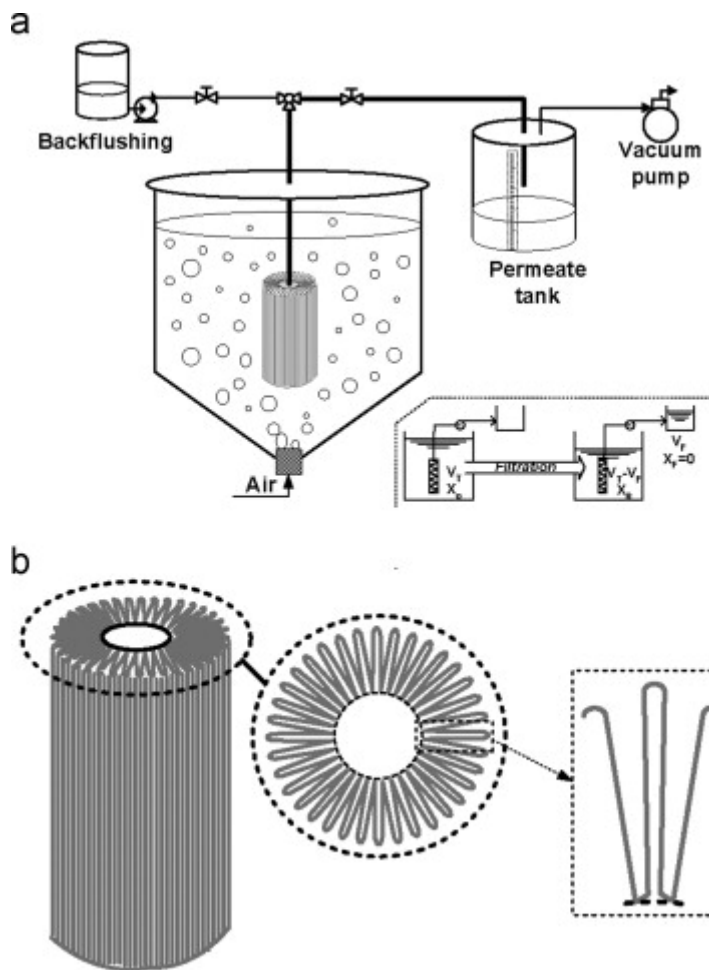


Fig. 1. Filtration equipment (a) and structure of the pleated cartridge (b).

Biofouling, generically defined as the deleterious attachment of bacteria cells and extracellular polymeric substances (EPS) to a solid surface, has been regarded as one of the main obstacles to efficient use of microfiltration processes [4]. Once membrane fouling occurs, it will reduce permeate flux, increase feed pressure, reduce productivity, increase system downtime, increase membrane maintenance and operation costs due to membrane cleaning, and decrease the lifespan of the membrane modules. The fouling can occur by pore blocking, pore constriction, caking or a combination of the mechanisms [5], [6].

Frequently, cartridges are not cleanable and so can only be used once; after their dirt loading capacity has been reached or the pressure loss across them has become unacceptably high, the cartridge must be removed from the system being cleaned and disposed of by incineration, by disposal at a landfill site, or by some other means. However, disposal costs for used cartridges are generally about half of the purchase price. Disposal cost of cartridge filters used in hazardous applications can easily exceed the purchase price [7]. Recently there has been an increasing interest in the design of filter cartridges that have a lower environmental impact through their

use and disposal due to, for example, their reduced weight and alternative materials of construction and reduced disposal costs. [8].

In accordance with the previously exposed considerations, the better understanding of the fouling mechanism on microfiltration cartridge is the prime objective to develop strategies that increase the lifespan of the cartridge manipulating the process conditions and/or optimizing the cleaning protocols. Over the past few years, considerable investigations have been performed in order to provide a more detailed information about the fouling behavior, fouling factors and fouling control strategies under dead-end flow mode or in a wide range of membrane geometries (i.e. flat sheet, hollow fiber, tubular, and spiral wound) [9], [10], [11]. However, the studies about the fouling on microfiltration cartridges are scarce and they are mainly focused on the filtration of seawater [12], [13] or on the design of hydrodynamic models [8], [14], [15], but there is no information about the fouling of microfiltration cartridges in biotechnical applications, where high microorganism concentrations are frequent.

The aim of this work was therefore to study the characteristics and mechanisms of the fouling of microfiltration pleated cartridges in biotechnical applications, in order to obtain information about strategies that allow to increase its lifespan. Specifically, well-controlled pilot-plant scale fouling experiments were carried out using the biodegradation of salicylic acid by means of *Pseudomonas putida* as model of cellular media.

2. Materials and methods

2.1. Microorganism and culture medium

Fouling experiments were carried out with a culture of *Pseudomonas putida* DMS 4478 (DSMZ, German Resource Centre for Biological Material). This strain contains the SAL plasmid that encodes genes for the degradation of salicylate. The stock cultures were stored at 4 °C in nutrient agar slants, supplemented with salicylic acid.

The composition of nutrient medium in g/L was beef extract (3), peptone (5) and mineral salt medium (MSM). Mineral salt medium consisted of (g/L) KH_2PO_4 (0.422), K_2HPO_4 (0.375), $(\text{NH}_4)_2\text{SO}_4$ (0.244), $\text{MgSO}_4 \cdot 7\text{H}_2\text{O}$ (0.05), $\text{NH}_3 \cdot \text{Fe} \cdot \text{Citrate}$ (0.054), NaCl (0.015), $\text{CaCl}_2 \cdot 12\text{H}_2\text{O}$ (0.015) and tryptone (0.05). pH was adjusted to 7. Prior to use, nutrient medium, MSM, pipettes and other material, were autoclaved at 121° for 20 min.

The bioprocess feed was prepared by dissolving salicylic acid (Panreac, Spain) in MSM, with tap water, at desired concentration.

2.2. Free suspension cultivation

Previously of inoculation in bioreactor tank, *Pseudomonas putida* was grown in nutrient medium supplemented with 100 mg/L of salicylic acid, at 30 °C, for cellular activation, as follows. Isolated colonies of *Pseudomonas putida* were inoculated in 250 mL of nutrient medium supplemented with salicylic acid in 500 Erlenmeyer flasks. Prior to inoculation in the bioreactor, cells were harvested during the final exponential growth phase and centrifuged at 6000 rpm at 4 °C during 30 min. The dried cells were subsequently resuspended in MSM. The initial cellular concentration in the bioreactor after inoculation was 0.023 g/L (corresponding of 1.5×10^7 cfu/mL).

2.3. Filtration equipment

The experiments were carried out in a 20 L bioreactor (Fig. 1a) with 13 L of working volume, equipped with an aeration system composed by an air diffuser installed on the bottom of the bioreactor. Air flow rate varied between 400 and 450 mL/min, in order to provide biological oxygen requirements and maintaining biomass in suspension. Bioreactor is cover by a lid to prevent contamination. Inside the bioreactor, there was introduced a 10-inch microfiltration PES pleated cartridge, with a pore size of 0.2 μm , and a total membrane area of 0.78 m² (LifeAssure PDA CUNO/3 M), whose characteristic are listed in Table 1. To promote the effect of air bubbles on membrane surface, polypropylene core was removed. Bioreactor was fed with synthetic salicylic acid wastewater through a peristaltic pump (Masterflex I/P 77601-10) and permeate was collected in a 26 L tank by a vacuum pump. Backpulsing cycles were carried out with water trough a peristaltic pump (Masterflex L/S 7518-00).

Table 1. Membrane characteristics.

<i>Property</i>	Empty Cell
<i>Membrane material</i>	Polyethersulfone
<i>Membrane support layer</i>	Polypropylene
<i>Membrane configuration</i>	Pleated cartridge
<i>Filtration surface area</i>	0.78 m ²
<i>Pore size</i>	0.2 μm
<i>Maximum operation temperature</i>	80 °C

2.4. Chemical cleaning techniques

The cleaning protocol was performed as follows:

Rinse with hot water (1 h);

rinse with NaOH (2% w/v) solution (1 h) followed rising with water;

rinse with HNO₃ (0.5% w/v) solution (1 h);

rinse with water.

At the end of the cleaning, water permeability of the membrane was measured in order to check the efficiency of the method in membrane recovery.

2.5. Analytical methods

Suspended cell concentration in the bioreactor was determined by measuring the value of OD at 600 nm using the UV/visible spectrophotometer (UV-vis 1203, Shimadzu). Cell concentration was estimated from a correlation between OD and cell dry weight. One unit of OD was found to be equivalent to 0.451 g of cell dry weight per liter.

2.6. Scanning electron microscopic (SEM) images

Surface of the fouled membrane was analyzed by scanning electron microscopy using a JEOL-6100 scanning electron microscope (JEOL Ltd., Tokyo, Japan). Fresh membranes were dried in an oven during 24 h to ensure to be complete dried. When dry, membranes were mounted on aluminum stubs with double-sided carbon sticky tape, sputtered with gold in a vacuum evaporator (Balzers SCD 004, BAL-TEC AG), prior to observation under the SEM.

3. Results and discussion

3.1. Discontinuous filtration

The first 5 days were considered as an acclimatization period, in which *P. putida* was adapted to new environmental conditions. In this period, salicylic acid was added at different concentrations up to 1000 mg/L and there was not any filtration period, in order to increase the concentration of suspended biomass. Until a biomass concentration of around 1 gDCW/L was reached, bioreactor was operated during 15 days by means of discontinuous filtrations. Different quantities of permeate were drawn each day and fresh sterile medium was added to the bioreactor in order to maintain the volume of fluid. At the beginning of this period, 3 L of permeate were processed, increase up to 12 L at the end of the discontinuous step, in 3 L series.

As it can be seen in Fig. 2a, no decline in permeability (defined as $L_p = (1/A \cdot TMP) \left(\frac{dV_F}{dt} \right)$) was observed after the first 5 days of operation, which correspond with the acclimation period. This fact indicates that the growth of *P. putida* over the membrane surface before filtration is negligible. As it can be expected, when the filtration periods under constant pressure operation started (TMP: 0.13 bar), permeability declined due to the fouling. The flux reduction was initially fast. So, between the 5th and the 8th day, a permeability reduction of 80.7% was achieved, which correspond with a cumulative filtered volume of 18 L (around 1.4 times the volume of the tank). It was also observed that the no increase of the flux after the non-filtration periods, which will be explained later. Non-filtration periods correspond to the time between consecutive filtrations (see horizontal dotted lines for evolution of VF in Fig. 2a). Finally, between 8th and 14th day, the flux decay was less severe, achieving a final permeability of around 170 L/m² h bar after the filtration of 45 L (3.5 times the volume of the tank).

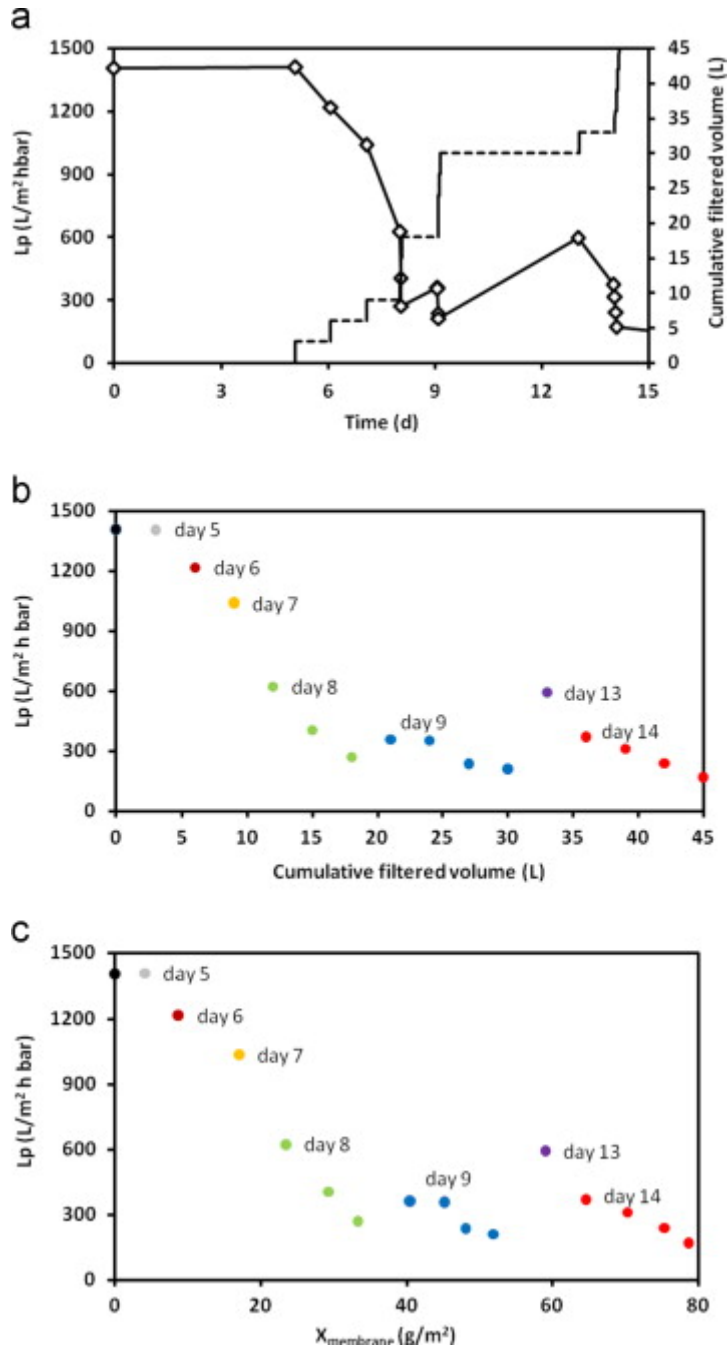


Fig. 2. (a) Evolution of permeability (\diamond) and cumulative filtered volume (dotted line) during discontinuous filtrations. (b) Evolution of permeability in front of the cumulative filtered volume during the discontinuous filtrations. (c) Evolution of permeability in front of the theoretical attached biomass to membrane during the discontinuous filtrations.

Comparing permeability and cumulative filtered volume (Fig. 2b), it can be observed a linear relationship between the filtered volume and the permeability reduction during the filtration of the first 20 l, even when this volume was discontinuously filtered. In order to explain this behavior, theoretical concentration of solids on the membrane surface ($\bar{X}_{membrane}$) was estimated using the formula below, where $X_{0,i}$ and $X_{R,i}$ are the solid concentrations in the tank before and after the filtration of day i , respectively:

$$\bar{X}_{membrane} = \sum_{i=day 5}^{i=day j} \frac{V_T X_{0,i} - (V_T - V_{R,i}) X_{R,i}}{A} [=] g/m^2 \quad (1)$$

It can be seen from Fig. 2c a linear relationship between the solids concentration in the membrane surface and the reduction of the permeability for $\bar{X}_{membrane}$ lower than 33 g/m². From this fact, two suggestions follow: first, the permeability is proportional to the amount of solids retained over the membrane surface, which indicates the formation of an incompressible cake layer or a complete blocking mechanism. Secondly, no improvement of the permeability was observed after the non-filtration periods, showing that the detachment of biomass from the surface of the membrane, mainly due to the air scouring, is negligible. This behavior could be due to the accumulation of biomass in the small spaces between pleats. The air bubbles are unable to penetrate into the pleated structure and to access these spaces due to their size, reducing the scour effect of the air on the attached biomass.

Assuming constant pressure, the specific membrane and cake resistances were determined by correlating cumulative filtered volumes (V_F) and required times of filtration (t) (non-filtration periods are here not taken into account) by means of Eq. (2):

$$t/V_F = \frac{2\mu\alpha X_S}{2A^2\Delta P} V_F + \frac{\mu R_M}{A\Delta P} = aV_F + b \quad (2)$$

where α and R_M are the specific membrane and cake resistances, μ is viscosity and X_S is the mass of solids in the cake per volume of filtrate (that is, $X_S = \bar{X}_{membrane}/V_F$). Specific resistances were determined to be $\alpha=3.08 \times 10^{13}$ m/kg and $R_M=2.24 \times 10^{11}$ m⁻¹ ($r^2=0.998$).

It is also remarkable that increases of the permeability during non-filtration periods were observed after the 8th day, that is, for $\bar{X}_{membrane}$ higher than 33 g/m². This fact suggests that the effect of the air scouring on the detachment of the solids of the surface membrane became more significant for high $\bar{X}_{membrane}$ values. A possible cause of this behavior can be that the spaces between pleats are completely covered by the fouling and the biomass begins to accumulate over the pleated structure, where the scour effect of the air bubbles is more intense (Fig. 3).

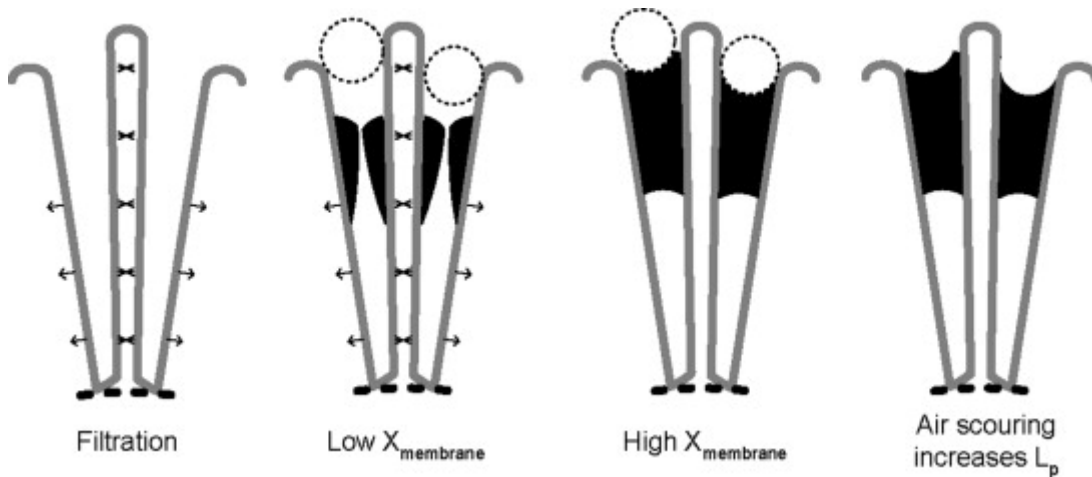


Fig. 3. Proposed effect of the air scouring on permeability at high solids concentration in the membrane surface.

3.2. Fouling control

3.2.1. Relaxation and backflushing

With the purpose of evaluating the mitigation of the fouling in microfiltration pleated cartridges by physical methods, continuous filtrations alternated with relaxation or backflushing periods were carried out after the 14th day (Fig. 4a) in order to maintain permeabilities higher than 50 L/m² h bar, which corresponds with a 4% of the initial permeability.

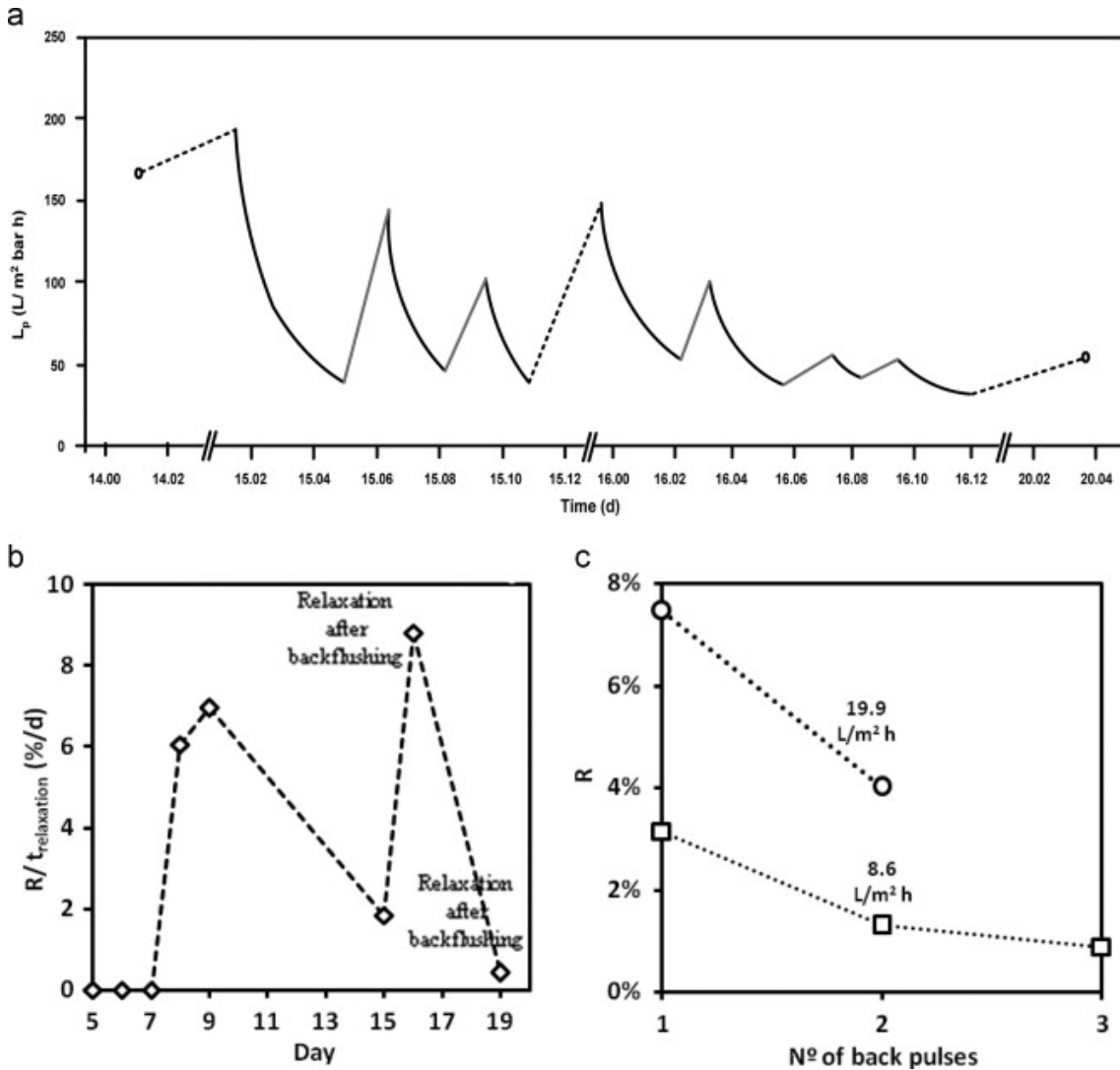


Fig. 4. Evolution of the permeability during the periods of continuous filtration (continuous line), relaxation (dotted line) and backflushing (gray line) (a). Recoveries of permeability obtained by means of relaxation (b). Effect of the backflux and number of back pulses on the recovery of permeability (back pulse duration: 30 s) (c).

Relaxation is simply ceasing permeation whilst continuing to scour the membrane with air bubbles. During filtration process, biomass was compressed on membrane surface due to drag force caused by suction. When filtration process stops, bacteria deposited on membrane surface could be removed by aeration turbulence. According to Fig. 4, only moderate improvements of the permeability due to air scouring were observed.

Fig. 4b shows the ratio permeability recovery to relaxation time obtained by air scouring during all the experiment. Permeability recovery was defined as:

$$R = \frac{L_{p,after\ cleaning} - L_{p,before\ cleaning}}{L_{p,initial}} \times 100 \quad (3)$$

During the last relaxation period (4 days), only a permeability recovery of around 1.6% was observed, indicating an irreversible character of the fouling of the pleated membrane at the end of the experiment [16]. As it was previously explained, the non-effect of the relaxation on the recovery during the first days was attributed to the accumulation of solids into the spaces between pleats. The permeability recovery observed after 8th day was caused by air scouring of the solids accumulated outside the filter. It must be pointed out that permeability recovery reached a maximum and then decreased, due to the accumulation of irreversible foulants. However, a significant increase of the permeability was observed during the relaxation after the first period of backflushing, which could be due to a partial detachment and or displacement of the biomass accumulated into the spaces between pleats towards the outer perimeter of the filter (Fig. 5). Due to this fact, the cleaning effect of the air scouring on this biomass was more effective.

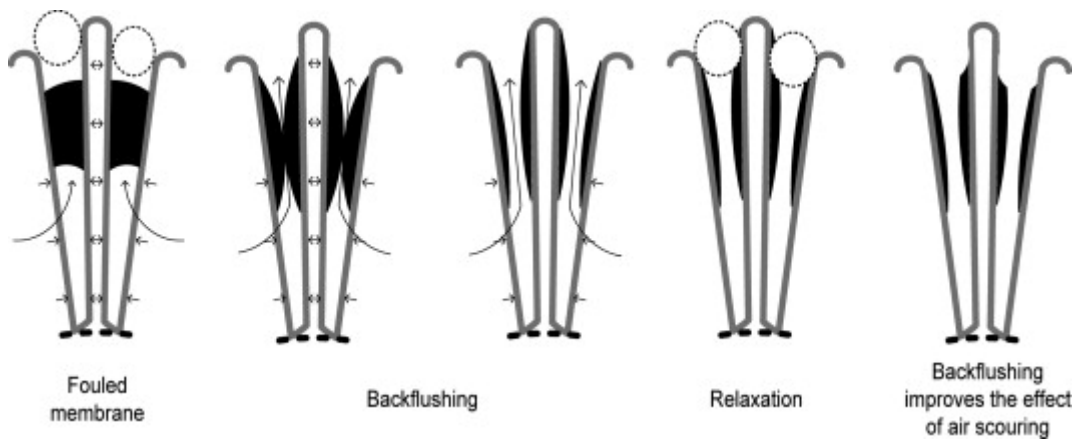


Fig. 5. Proposed effect of the consecutive application of backflushing and relaxation (air scouring) on permeability.

Backflushing is a process used to clean filters by reversing the flow of fluid through the system. This method has been found to successfully remove most of the reversible fouling due to pore blocking, transport it back into the bioreactor, and partially dislodge loosely attached sludge cake from the membrane surface. Two backfluxes were assayed: 19.9 and 8.6 L/m² h. The duration of each period of backflushing was 30 s and they were carried out when the permeability of the filter during the filtration reached a value near to 50 L/m² h bar. Periods of backflushing are shown as gray lines in Fig. 4a. As it can be observed, the fouling removal efficiency of this method was higher than the obtained using the relaxation. It is also worth mentioning that low flux and short backwash times (30 s) were employed during backflushing, which indicates that small amounts of the produced permeate were required for the cleaning of the membrane by means of this technique. From Fig. 4c, it can be noted that as the backflux was increased, the permeability increased, which is the expected behavior. As it can be also expected, backflushing effectiveness tended to decrease with operation time and consecutive applications, as more irreversible fouling accumulates on the membrane surface.

The increase of filter lifespan of around 2 days obtained by means of back flushing and relaxation periods is not as small as it might appear at first sight. It must be taken into account that the

filtered volume during these two days was 28 L (around 40% of the total filtered volume during all the experiment).

3.2.2. Chemical cleaning

At the end of the study, an intensive chemical cleaning was done in order to remove the irreversible fouling of the membrane and trying to restore initial permeate flux of the microfiltration pleated cartridge. Chemical cleaning was conducted according to the protocol indicated in the Material and methods section.

Fig. 6 shows water permeabilities of the new, fouled and cleaned cartridge. Results show a permeability recovery (R) of 87.8%, obtaining a final permeability after cleaning of the 95% of the initial value. In conclusion, the effectiveness of the assayed chemical cleaning protocol has been demonstrated, which allows a considerable increase of the lifespan of the cartridge.

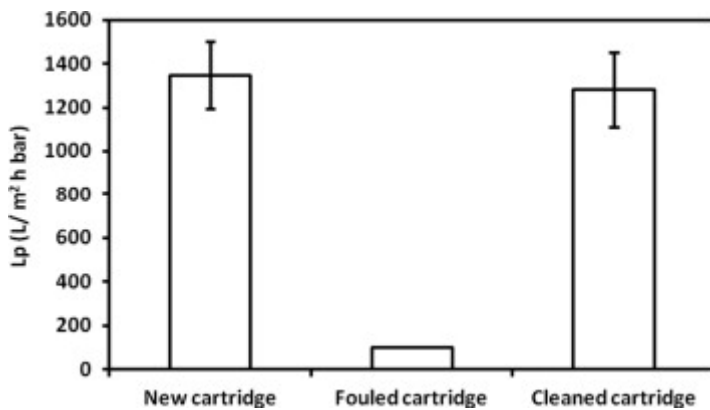


Fig. 6. Water permeabilities of the new, fouled and cleaned cartridge. Vertical lines denote standard deviations (n=4 except for fouled cartridge, for which no replicates were made).

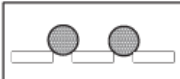
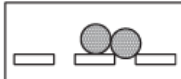
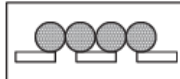
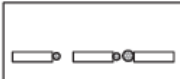
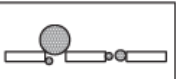
Based on the obtained results with the different methods for the fouling control, our recommendations for a “commercial operation sequence” are: (i) filtration; (ii) application of backflushing followed by relaxation when the permeability decays until to a limit value (backflushing increases the fouling removal efficiency of the relaxation); (iii) filtration and (iv) chemical cleaning of the pleated microfiltration cartridge when the limit value of permeability is reached again.

3.3. Fouling of the pleated microfiltration cartridge

3.3.1. Mechanism

In order to elucidate the fouling mechanism involved in the loss of permeability of the pleated membrane during the microfiltration of *P. putida*, data of permeate volumes versus time of filtration obtained during the 15th day of experimentation (exactly before the first backflushing period), were fitted using the individual and combined fouling models proposed by Bolton et al. [5]. The best fit was determined by minimizing the sum of squared residuals (SSR) where residual was equal to the difference between a data point and the model prediction. Table 2 shows a brief description of the simple mechanisms of membrane fouling, the fitted parameters of the models and the SRR values for each model whereas the data and the model fits are compared in Fig. 7.

Table 2. Main mechanisms of fouling: brief description, fitted parameters and SRR obtained using the experimental data.

Model	Complete blocking	Intermediate blocking	Cake filtration	Standard blocking	Complete- standard blocking
Figure					
Description	Particles seal off pore entrances	A portion of the particles seal off pores and the rest accumulate on the top of other deposited particles.	Particles accumulate on the surface of the membrane in a permeable cake of increasing thickness	Particles accumulate inside membrane on the walls of straight cylindrical pores	Simultaneous fouling by means of complete and standard mechanisms
Model	$V = \frac{J_0}{K_b} \cdot (1 - \exp(-K_b t))$	$V = \frac{1}{K_i} \cdot \ln(1 + K_i J_0 t)$	$V = \frac{1}{K_c J_0} \cdot (\sqrt{1 + 2K_c J_0^2 t} - 1)$	$V = \left(\frac{1}{J_0 t} + \frac{K_s}{2} \right)^{-1}$	$V = \frac{J_0}{K_b} \cdot \left(1 - \exp\left(\frac{-2K_s t}{2 + K_s J_0 t} \right) \right)$
Parameters	$K_b = 3.91 \times 10^{-4} \text{ s}^{-1}$	$K_i = 132.2 \text{ m}^{-1}$	$K_c = 4.4 \times 10^7 \text{ s/m}^2$	$K_s = 109.1 \text{ m}^{-1}$	$K_b = 3.92 \times 10^{-4} \text{ s}^{-1}$ $K_s = 3.63 \times 10^{-6} \text{ m}^{-1}$
SRR	1.22×10^{-7}	5.58×10^{-7}	1.20×10^{-6}	2.93×10^{-7}	1.23×10^{-7}
r^2	0.9995	0.995	0.98	0.997	0.9994

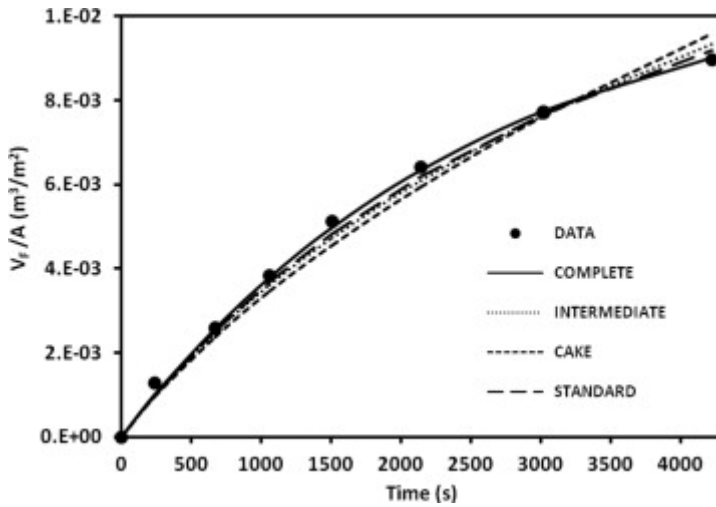


Fig. 7. Volume vs. time data compared to the complete model, intermediate model, cake model and standard model predictions.

The best fit of the data occurred with the complete blocking model, which had a SRR value slightly lower than the standard blocking model, which suggests that the particles seal off pore entrances and prevent flow. Table 2 also includes a fouling model that accounted for the combined effects of the complete and standard blocking [5]. The contributions of standard blocking and intermediate blocking to the combined model were evaluated from the values of K_b and K_s . The high value of the ratio $K_b/(K_s J_0)$ seems to corroborate that complete blocking mechanism had the major contribution.

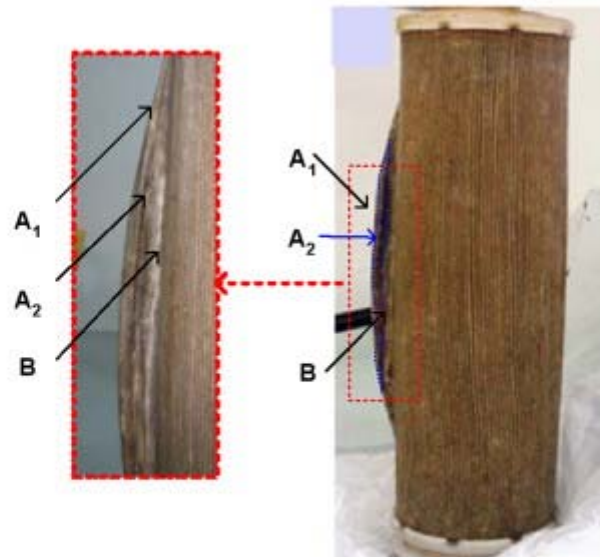
3.3.2. SEM imaging of the pleated membrane

To better understand how is the bacterial deposition on the membrane surface and into the pleated structure, the fouled membrane was withdrawn from the bioreactor at the end of the experiment and photographs and SEM images of different regions of the membrane were taken to illustrate the deposition patterns of cells along the cartridge surface.

Fig. 8 shows the non-uniform distribution of the fouling on the surface of the pleated membrane. Three regions were distinguished: the area near the peak of the pleat (A_1 ; around 25% of the total area), where the fouling rate is high due to the easy access of the bacteria but also where the effect of the air scouring is more effective; the adjacent area (A_2 ; around 60% of the total area), which showed the highest fouling because air bubbles can not introduce into the pleated

structure; and a relatively clean area at the base of the pleat (B; around 15% of the total area), in which the accessibility of bacteria was the lowest. In this sense, Brown et al. [17] also visualized the different accessibility of micro-sized particles into the pleated structure of the cartridge during filtration of diluted yeast suspensions. They observed a range of clean and fouled membrane areas related to the open pleat structure of the pleat pack density.

a



b

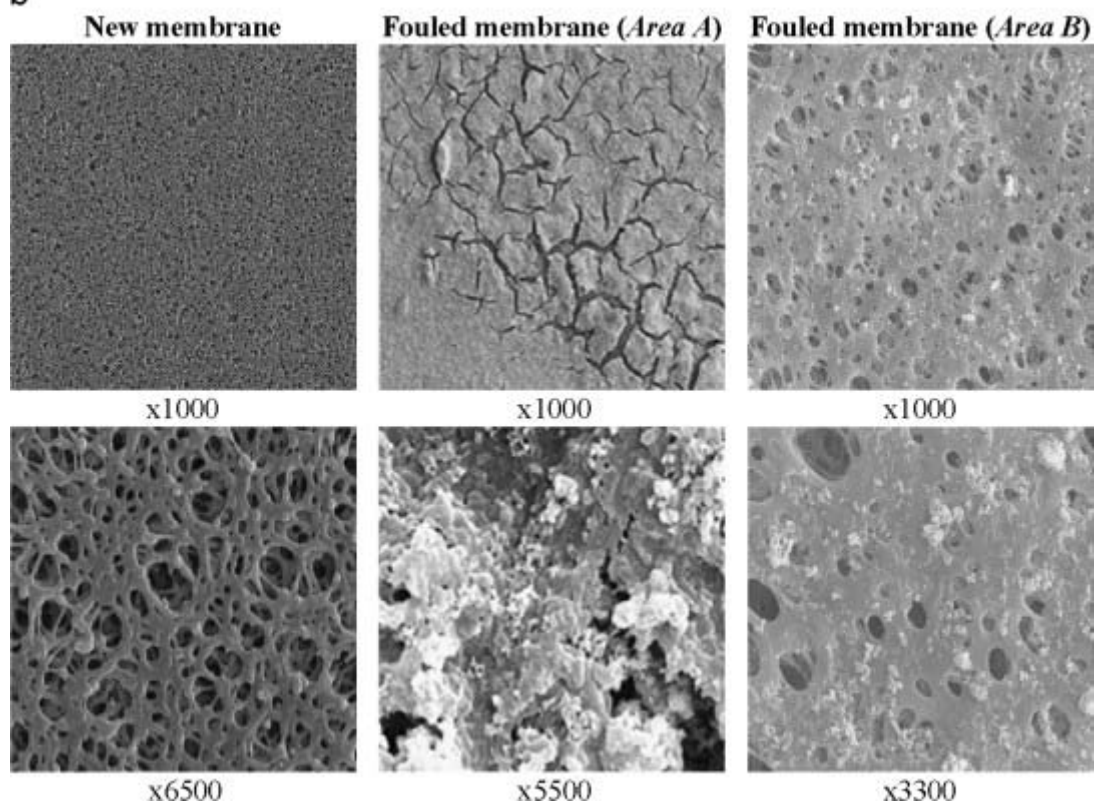


Fig. 8. Observed non-uniform distribution of the fouling on the surface of the pleated membrane (a). Scanning electron micrographs of the new membrane and the fouled membrane (b).

Micrographs from area B show that this zone is predominately clean. This fact is due to the fouling accumulated in area A₂, which acts as a barrier retaining cells. In the same manner, the pleat packing density reduces the capacity of the cells to deposit inside the pleats. It is also worth noting that particles deposited in this area of the surface of the membrane seem to have a diameter lower than the pore size.

Fig. 8b shows micrographs of the area A of the membrane. The fouling of this area is clearly higher than that of the observed one in the area B. It can be observed the presence of a practically continuous layer of fouling in this area, which is mainly responsible of the permeability decrease due to the complete blocking of the pores of the membrane. It must be taken into account that permeate fluxes (that is V_f/A) used for the fitting of the data to the different fouling models (Table 2 and Fig. 7) were defined employing the total membrane surface area and not the effective filtration area, (zone A), which can not be exactly determined. Obviously, this fact implies that the obtained fitting parameters (K_c , K_i , K_s and K_b) are based on total membrane surface (area A+area B).

4. Conclusions

The characteristics and mechanisms of the fouling of microfiltration pleated cartridges in biotechnical applications have been studied, using the degradation of salicylic acid by *Pseudomonas putida* as model bioprocess.

Discontinuous filtrations showed an initial linear relation between the decrease of flux and the volume of permeate and a null effect of the air scouring on the permeability recovery. This behavior was attributed to the accumulation of solids into the spaces between pleats, where the access of the bubbles is complicated. For higher concentration of solids on the membrane surface ($\bar{X}_{membrane} > 33 \text{ g/m}^2$), moderate permeability recoveries were observed after relaxation periods of days or after backflushing. In both cases, effectiveness tended to decrease with operation time and consecutive applications of these techniques, as more irreversible fouling accumulates on the membrane surface. However, the permeability recovery by means of relaxation was improved when a previous backflushing was carried out. By chemical cleaning, a recovery of the initial flux of around 95% was obtained, suggesting an efficient method to restore the permeability lost during the biotechnical process and increase the lifespan of the cartridge.

A non-uniform distribution of the fouling in the cartridge was observed, concluding that the main accumulation of fouling occurs into the spaces between pleats near the outside of the filter, forming a layer that also reduced the fouling into the pleated structure. The evaluation of different fouling models shows that a complete model provided the best fit to the experimental data, concluding that the fouling behavior were more consistent with the gradual pore blocking by large particles of the membrane area near of the peak of the pleat.

Acknowledgments

This work was financially supported by the MICINN (Spanish Ministry of Science and Innovation) within the Project CTM2007-66216. I.R. was the recipient of a fellowship from MICINN (Spanish Ministry of Science and Innovation, Spain). The authors would like to thank the Scanning Electron Microscopy service of the University of Oviedo for the provided assistance.

References:

- [1] APHA. Standard Methods for the Examination of Water and Wastewater. American Public Health Association, Washington, DC (2005).
- [2] Â.C. Apolinário, A.M.T. Silva, B.F. Machado, H.T. Gomes, P.P. Araújo, J.L. Figueiredo, J.L. Faria. Wet air oxidation of nitro-aromatic compounds: reactivity on single- and multi-component systems and surface chemistry studies with a carbon xerogel. *Applied Catalysis B: Environmental*, 84 (2008), pp. 75-86.
- [3] S.K. Bhargava, J. Tardio, J. Prasad, K. Föger, D.B. Akolekar, S.C. Grocott. Wet oxidation and catalytic wet oxidation. *Industrial & Engineering Chemistry Research*, 45 (2006), pp. 1221-1258.
- [4] M.J. Birchmeier, C.G. Hill, C.J. Houtman, R.H. Atalla, I.A. Weinstock. Enhanced wet air oxidation: synergistic rate acceleration upon effluent recirculation. *Industrial & Engineering Chemistry Research*, 39 (2000), pp. 55-64.
- [5] L.T. Boock, M.T. Klein. Experimental kinetics and mechanistic modeling of the oxidation of simple mixtures in near-critical water. *Industrial & Engineering Chemistry Research*, 33 (1994), pp. 2554-2562.
- [6] S. Collado, D. Quero, A. Laca, M. Díaz. Fe²⁺-catalyzed wet oxidation of phenolic acids under different pH values. *Industrial & Engineering Chemistry Research*, 49 (2010), pp. 12405-12413.
- [7] S. Collado, L. Garrido, A. Laca, M. Díaz. Wet oxidation of salicylic acid solutions. *Environmental Science & Technology*, 44 (2010), pp. 8629-8635.
- [8] D. Fu, J. Chen, X. Liang. Wet air oxidation of nitrobenzene enhanced by phenol. *Chemosphere*, 59 (2005), pp. 905-908.
- [9] Y.-C. Hsu, H.-C. Yang, J.-H. Chen. The enhancement of the biodegradability of phenolic solution using preozonation based on high ozone utilization. *Chemosphere*, 56 (2004), pp. 149-158.
- [10] N. Kulik, M. Trapido, A. Goi, Y. Veressinina, R. Munter. Combined chemical treatment of pharmaceutical effluents from medical ointment production. *Chemosphere*, 70 (2008), pp. 1525-1531.
- [11] T. Mandal, S. Maity, D. Dasgupta, S. Datta. Advanced oxidation process and biotreatment: their roles in combined industrial wastewater treatment. *Desalination*, 250 (2010), pp. 87-94.
- [12] V.S. Mishra, V.V. Mahajani, J.B. Joshi. Wet air oxidation. *Industrial & Engineering Chemistry Research*, 34 (1995), pp. 2-48.
- [13] D.P. Mohapatra, S.K. Brar, R.D. Tyagi, R.Y. Surampalli. Physico-chemical pre-treatment and biotransformation of wastewater and wastewater sludge – Fate of bisphenol A. *Chemosphere*, 78 (2010), pp. 923-941.
- [14] J.B. Quintana, S. Weiss, T. Reemtsma. Pathways and metabolites of microbial degradation of selected acidic pharmaceuticals and their occurrence in municipal wastewater treated by a membrane bioreactor. *Water Research*, 39 (2005), pp. 2654-2664.
 - A. Santos, P. Yustos, A. Quintanilla, F. García-Ochoa, J.A. Casas, J.J. Rodríguez. Evolution of toxicity upon wet catalytic oxidation of phenol. *Environmental Science & Technology*, 38 (2003), pp. 133-138.
- [15] R.V. Shende, J. Levec. Wet oxidation kinetics of refractory low molecular mass carboxylic acids. *Industrial & Engineering Chemistry Research*, 38 (1999), pp. 3830-3837.
- [16] M.E. Suarez-Ojeda, A. Guisasola, J.A. Baeza, A. Fabregat, F. Stüber, A. Fortuny, J. Font, J. Carrera. Integrated catalytic wet air oxidation and aerobic biological treatment in a

- municipal WWTP of a high-strength o-cresol wastewater. *Chemosphere*, 66 (2007), pp. 2096-2105.
- [17] J. Vicente, R. Rosal, M. Díaz. Nuncatalytic oxidation of phenol in aqueous solutions. *Industrial & Engineering Chemistry Research*, 41 (2002), pp. 46-51.
- [18] J. Vicente, M. Díaz. Thiocyanate/phenol wet oxidation interactions. *Environmental Science & Technology*, 37 (2003), pp. 1457-1462.
- [19] R.S. Willms, D.D. Reible, D.M. Wetzel, D.P. Harrison. Aqueous-phase oxidation: rate enhancement studies. *Industrial & Engineering Chemistry Research*, 26 (1987), pp. 606-612.